Hindawi Publishing Corporation
International Journal of Photoenergy
Volume 2013, Article ID 364638, 6 pages
http://dx.doi.org/10.1155/2013/364638

Research Article

The Effect of Bandgap Graded Absorber on the Performance of a-$Si_{1-x}Ge_x$:H Single-Junction Cells with μc-SiO_x:H *N*-Type Layer

Hung-Jung Hsu, Cheng-Hang Hsu, and Chuang-Chuang Tsai

Department of Photonics, National Chiao Tung University, 1001 University Road, Hsinchu 300, Taiwan

Correspondence should be addressed to Hung-Jung Hsu; bear0300022@gmail.com

Received 27 July 2013; Revised 24 October 2013; Accepted 28 October 2013

Academic Editor: Gaetano Di Marco

We reported the effect of bandgap grading of absorbers on the performance of a-$Si_{1-x}Ge_x$:H cells employing μc-SiO_x:H *n*-layer. The influence of bandgap grading widths extended from the *p*-layer (the *p/i* grading) and the *n*-layer (the *i/n* grading) to the absorber on the cell performance which were systematically studied. The *p/i* grading reduced the interface defects and thus improved the V_{OC}. The reduced J_{SC} and FF were presumably due to the degraded hole transport by the potential gradient of *p/i* grading. Increasing the *i/n* grading width improved the carrier collection significantly. The EQE, the J_{SC}, and the FF were improved substantially. Bias-dependent EQE revealed that the carrier collection is efficient in the cell employing optimal *i/n* grading. On the other hand, increasing the *i/n* grading width was accompanied by the decrease in long-wavelength response which potentially constrained the *i/n* grading width. Compared to the cell without grading, the a-$Si_{1-x}Ge_x$:H cells with optimal *p/i* and *i/n* grading width improved the efficiency from 5.5 to 7.5%.

1. Introduction

Hydrogenated amorphous silicon germanium (a-$Si_{1-x}Ge_x$:H) has been shown to be a promising material for low-bandgap absorber in the multijunction structure [1]. Yan et al. reported that an initial efficiency over 16% was achieved by using a-Si:H/a-$Si_{1-x}Ge_x$:H/nc-Si:H triple-stacked structure and by employing *n*-type microcrystalline silicon oxide (μc-SiO_x:H(*n*)) as the *n*-layer for each subcell [2]. The μc-SiO_x:H(*n*) has larger bandgap and lower refractive index compared to conventional amorphous or microcrystalline silicon *n*-layer, which reduced the parasitic absorption loss and increased the current density of component cell due to internal reflection, respectively [3, 4]. Moreover, the μc-SiO_x:H(*n*) has been intensively studied for the application as the intermediate reflecting layer between component cells [5, 6], as the window layer in the *n*-side illuminated μc-Si:H single-junction cells [7], and as the back reflector in a-Si:H single-junction cells [8]. We also found that the μc-SiO_x:H(*n*) functioned well as back reflector in a-$Si_{1-x}Ge_x$:H single-junction cells in our previous work [9]. This functional μc-SiO_x:H *n*-layer can significantly improve the performance of single- and multijunction cells.

On the other hand, one of the major challenges in developing a-$Si_{1-x}Ge_x$:H solar cells is the defective interfaces between the low-bandgap a-$Si_{1-x}Ge_x$:H absorber and the doped layers, which deteriorated, cell performance significantly. The *p/i* and the *i/n* interfaces contained considerable defects due to sharp changes in material composition [4]. The situation is even worse at the interface between the undoped a-$Si_{1-x}Ge_x$:H and *n*-type μc-SiO_x:H. High defect density at the interfaces increases the carrier recombination loss and weakened the built-in electric field in the absorber, which leads to the decrease in V_{OC}, J_{SC}, and FF. Guha et al. have reported that the employment of bandgap graded layers in the absorber can facilitate carrier collection, strengthen the built-in electric field, and thus improve the cell efficiency [10]. Several groups have reported the optimized bandgap grading structure in a-$Si_{1-x}Ge_x$:H absorber with a-Si:H *n*-layer through numerical simulation approaches [11–16]. However, there are still possibilities in designing the graded bandgap structure.

In this work, we systematically investigated the effect of bandgap grading widths on the performance and spectral responses of a-$Si_{1-x}Ge_x$:H cells with μc-SiO_x:H(*n*) as *n*-layer.

The biased quantum efficiency serves as an important tool in the investigation of carrier collection losses in a-$Si_{1-x}Ge_x$:H single-junction cells [15]. This approach would give us physical insight into the correlation among carrier collection, carrier generation, and bandgap grading width in the absorber.

2. Materials and Methods

Silicon-based thin films were prepared in a 27.12 MHz single-chamber PECVD system with a load-lock and a transfer chamber. Gas mixture of SiH_4, GeH_4, CO_2, B_2H_6, PH_3, and H_2 was used as source gases. *N*-type μc-SiO_x:H layer was prepared under power of 30 W and CO_2-to-SiH_4 flow ratio of 0.54. The resulting refractive index (at wavelength of 650 nm) and the optical bandgap, E_{04} (photon energy where the absorption coefficient is 10^4 cm^{-1}), were 3.2 and 2.2 eV, respectively. The a-$Si_{1-x}Ge_x$:H single-junction solar cells were deposited on the SnO_2:F coated glass substrates in a *p-i-n* superstrate configuration. The bandgap graded absorber was prepared by continuously varying the germane-to-silane flow rate ratio during the deposition process while maintaining the total thickness of the absorber at 230 nm. The bandgap graded layers were extended from the *p/i* and *i/n* interfaces toward the middle of the absorber with the bandgap changed from 1.75 to 1.53 eV. Photoconductivities of the bandgap graded layers decreased from 1.2×10^{-5} to 3.1×10^{-6} S/cm while the dark conductivities are quite similar ($\sim 4 \times 10^{-10}$ S/cm) with decreasing the bandgap from 1.75 to 1.53 eV. After the deposition, the cells were transferred to a sputter chamber to deposit the ITO/Ag back contacts.

The bandgaps were obtained by analyzing the transmittance and reflection spectra of a-$Si_{1-x}Ge_x$:H films using Tauc's method [17]. The optical reflection of cells was measured by UV/VIS spectroscopy. The external quantum efficiency (EQE) was characterized under both short-circuit and voltage-biased conditions. The *J-V* characteristics of a-$Si_{1-x}Ge_x$:H single-junction solar cells were obtained from the *J-V* measurement under illumination of AM1.5G light source with the electrode area of 0.25 cm^2.

3. Results and Discussion

3.1. Inefficient Carrier Collection in a-$Si_{1-x}Ge_x$:H Single-Junction Cells with Single-Bandgap Absorber. Figure 1 shows the external quantum efficiency (EQE) of a-$Si_{1-x}Ge_x$:H single-junction cells measured under different reverse biases. Bandgap graded layers were not employed in this cell. As the bias voltage increased from 0 to −0.5 V, the EQE increased significantly in longer wavelength region (>450 nm). Further increase in bias voltage from −1.0 to −1.5 V had only marginal enhancement in EQE which indicated that most carriers were extracted from the device. The difference in EQE between 0 and −1.5 V revealed that the carrier collection is inefficient in a-$Si_{1-x}Ge_x$:H cells using single-bandgap absorber. We believed that the asymmetric EQE enhancement is due to the inefficient hole collection coming from the low drift mobility of holes in amorphous material. Both the bulk defects and interface defects can trap carriers and hinder photogenerated carriers from being collected. Moreover, trapped carriers can

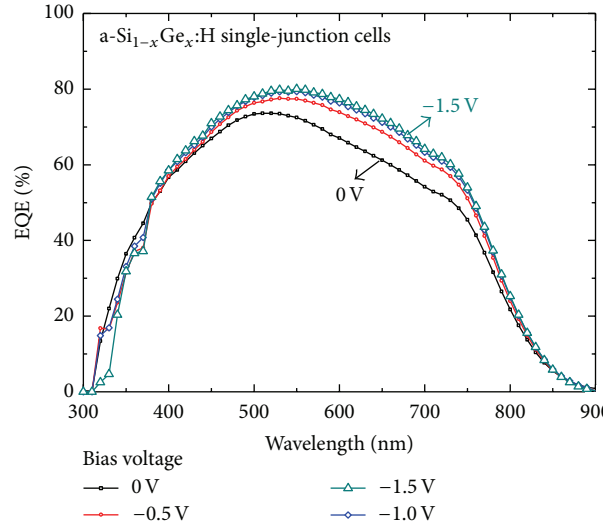

FIGURE 1: External quantum efficiency (EQE) of a-$Si_{1-x}Ge_x$:H single-junction cells with different reverse biases. The bias voltage was changed from 0 to −1.5 V.

weaken the built-in electric field in the middle of the absorber which worsened the carrier collection efficiency. To mitigate the detrimental effect of the inefficient carrier collection in the single-bandgap absorber, we employ the bandgap graded layers extended from the *p/i* and the *i/n* interfaces toward the middle of the absorber. The effect of *p/i* and *i/n* grading widths on cell performance was systematically studied.

The schematic band structures of a-$Si_{1-x}Ge_x$:H single-junction solar cells without and with bandgap grading at the *p/i* and the *i/n* interfaces were illustrated in Figures 2(a) and 2(b). The valence and the conduction band were assumed to shift equally as the film Ge content varied in the bandgap graded layer. The lowest bandgap of a-$Si_{1-x}Ge_x$:H undoped-layer was 1.53 eV, while the a-Si:H *p*-layer and μc-SiO_x:H *n*-layer had bandgaps of 1.75 eV and 1.1 eV, respectively. The bandgap of μc-SiO_x:H *n*-layer was approximately 1.1 eV because of its microcrystalline nature and the low oxygen (~4 at.%) we used. The bandgaps of the bandgap graded layers were changed from 1.75 to 1.53 eV. To investigate the appropriate bandgap grading structure, the *p/i* grading width was varied from 0 to 70 nm and the *i/n* grading width was varied from 0 to 180 nm. The total thickness of a-$Si_{1-x}Ge_x$:H was fixed at 230 nm for every cell presented.

3.2. The Effect of p/i Grading Width on the Performance of a-$Si_{1-x}Ge_x$:H Single-Junction Cells. Figure 3 illustrates the absorptance (*A*) and EQE of a-$Si_{1-x}Ge_x$:H single-junction cells as a function of the *p/i* grading width. The EQEs were measured under 0 and −0.5 V bias voltages. For EQEs measured under short-circuit condition (0 V), increasing the *p/i* grading width from 0 to 20 nm reduced the EQE at wavelength from 700 to 800 nm. Since the absorptance of cells had no noticeable change in this region, the decrease in EQE can be attributed to the degradation of carrier collection. Presumably, the degraded hole collection was responsible for the reduced EQE [10–12]. Holes generated by long-wavelength

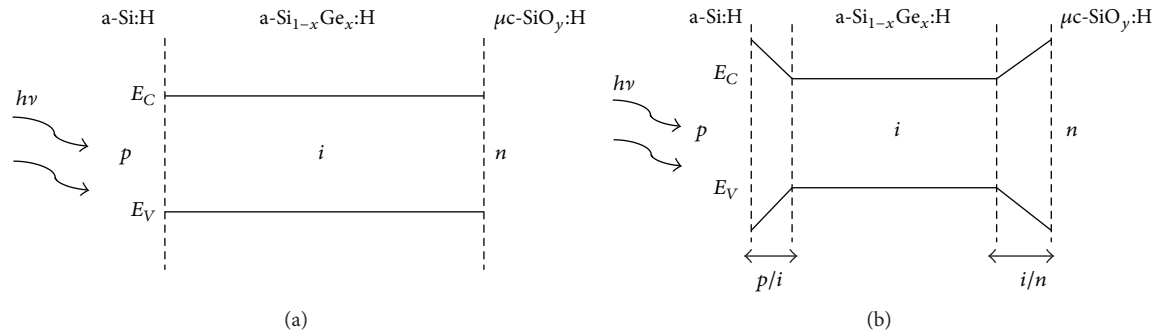

FIGURE 2: The schematic band structure of a-Si$_{1-x}$Ge$_x$:H single-junction cell (a) without bandgap grading and (b) with bandgap grading at both the p/i and the i/n interfaces.

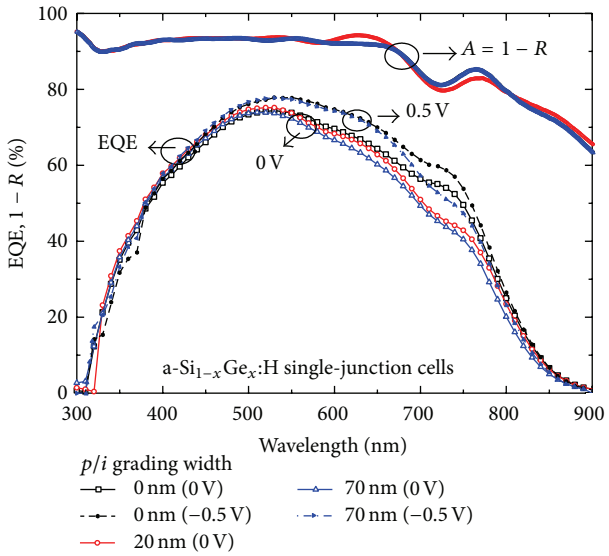

FIGURE 3: Absorptance (A) and EQE of a-Si$_{1-x}$Ge$_x$:H single-junction cells measured with 0 V and −0.5 V biases as a function of the p/i grading width. The p/i grading width was changed from 0 to 70 nm meanwhile keeping the total thickness of the absorber as 230 nm for all the cells.

photons near back contact would travel longer distance before being collected than the generated electrons. The potential gradient created by the p/i grading would hinder the hole transport which made the hole collection more difficult. Further increase in the p/i grading width to 70 nm reduced the EQE from 550 to 900 nm, which revealed that the hole collection was further degraded.

Table 1 summarizes the difference of current densities (ΔJ) measured with bias voltages of 0 and −0.5 V in EQE as a function of the p/i grading width. The ΔJ increased from 1.07 to 1.40 mA/cm^2 as the p/i grading width increased from 0 to 70 nm. The increased ΔJ manifested that the p/i grading degraded the carrier collection.

The performance of a-Si$_{1-x}$Ge$_x$:H single-junction cells with different p/i grading width was demonstrated in Figure 4. The short-circuit current (J_{SC}) and FF were slightly decreased as the p/i grading width increased from 0 to 20 nm.

TABLE 1: The reverse saturation current (J_0) and the difference of current densities (ΔJ) measured with bias voltages of 0 and −0.5 V in EQE as a function of the p/i grading width.

p/i grading width (nm)	0	20	70
ΔJ ($J_{EQE(-0.5\,V)} - J_{EQE(0\,V)}$) (mA/cm^2)	1.07	1.44	1.40
J_0 (A)	2.8×10^{-8}	1.3×10^{-9}	2.9×10^{-9}

Further increase in the grading width to 70 nm reduced the J_{SC} and the FF to 14.6 mA/cm^2 and 0.50, respectively. The reduction in the J_{SC} and the FF as the grading width increased from 0 to 70 nm was due to the degraded hole transport arising from the reduced potential gradient created by the p/i grading.

On the other hand, as the p/i grading width increased from 0 to 20 nm, the open-circuit voltage (V_{OC}) increased from 0.63 to 0.67 V. Further increase in the grading width to 70 nm increased the V_{OC} to 0.69 V. The improvement in V_{OC} may be due to the reduced defects at interfaces by bandgap graded layers [11, 12, 14]. Table 1 summarizes the reverse saturation current (J_0) of cells with different p/i grading width. As the grading width increased from 0 to 20 nm, the J_0 decreased approximately one order in magnitude from 2.8×10^{-8} to 1.3×10^{-9} A. The reduction in J_0 revealed that the defect density at the p/i interface was reduced by the bandgap graded layers, which improved the V_{OC}. In consequence, the thickness of the p/i grading width should be 10 to 20 nm to reduce the interface defects meanwhile minimizing the loss in J_{SC} and FF.

3.3. Effect of i/n Grading Width on the Performance of a-Si$_{1-x}$Ge$_x$:H Single-Junction Cells. Figure 5 illustrates the absorptance (A) and EQE of a-Si$_{1-x}$Ge$_x$:H cells with different i/n grading width. The p/i grading width and the total thickness of absorber were 15 and 230 nm, respectively, for all the cells. As the i/n grading width increased from 0 to 100 nm, the EQE at wavelength from 400 to 720 nm improved significantly. Since the absorptance had no obvious change from 400 to 720 nm, the increased EQE in this region can be attributed to the improved hole collection. Presumably, the potential gradient established by i/n grading facilitated

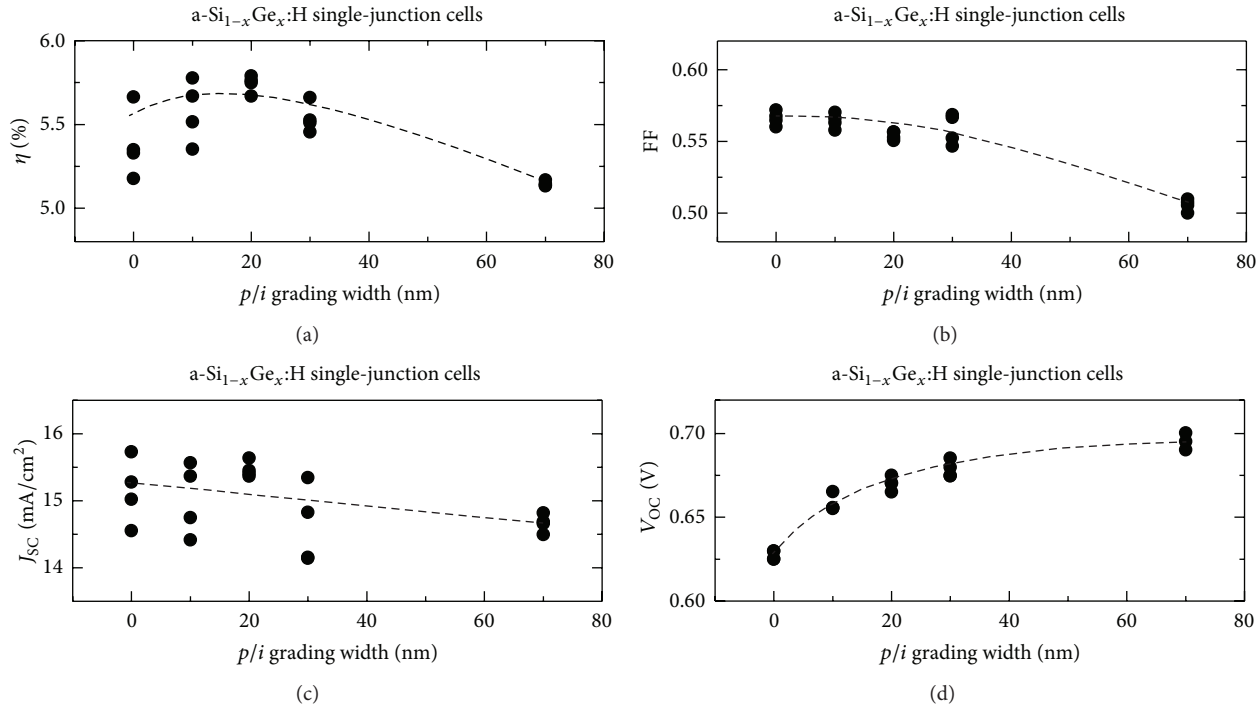

FIGURE 4: The performance of a-$Si_{1-x}Ge_x$:H single-junction cells as a function of the *p*/*i* grading width under illumination of AM1.5G light source. The *p*/*i* grading width was changed from 0 to 70 nm meanwhile keeping the total thickness of the absorber at 230 nm for all the cells. The lines were drawn to guide the eye.

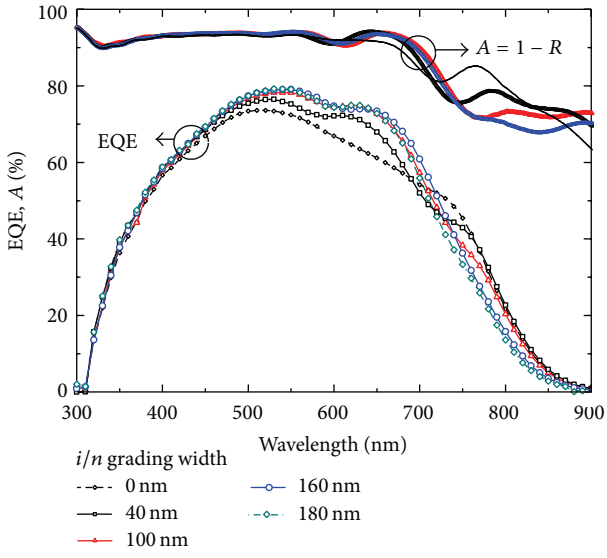

FIGURE 5: Absorptance (*A*) and EQE of a-$Si_{1-x}Ge_x$:H single-junction cells as a function of the *i*/*n* grading width. The *i*/*n* grading width was changed from 0 to 180 nm meanwhile keeping the *p*/*i* grading width and the total thickness of the absorber at 15 and 230 nm, respectively.

the hole transport. Also, the *i*/*n* grading modified the distribution of defects in the absorber which strengthened the built-in electric field that improved the carrier collection [11, 12, 14]. The reduction at the wavelength approximately 750 nm as the *i*/*n* grading width increased from 0 to 100 nm coincided with the decrease in absorptance in the same region, which was due to the reduction in carrier generation by the wider-bandgap graded layers.

As the *i*/*n* grading width increased from 100 to 160 nm, the EQE was further improved at wavelength from 650 to 750 nm while the EQE from 750 to 900 nm decreased noticeably. The former was due to the improved carrier collection while the latter, which coincided with the reduction in absorptance, revealed that the carrier generation was further reduced by wider bandgap graded absorbers. Further increase of *i*/*n* grading width to 180 nm reduced the EQE at the wavelength from 680 to 900 nm, which implied that the carrier generation was further suppressed.

The effect of the *i*/*n* grading width on the performance of a-$Si_{1-x}Ge_x$:H cells was demonstrated in Figure 6. As the *i*/*n* grading width increased from 0 to 180 nm, the V_{OC} increased monotonically from 0.66 to 0.69 V. The improvement in V_{OC} was due to the reduced defect density at the interfaces and the redistribution of defects in the absorber which strengthened the built-in electric field [11, 12, 14]. Since the *p*/*i* interface is the dominant junction for high V_{OC}, the modification of the *i*/*n* grading width had relatively smaller improvement on V_{OC} than the *p*/*i* grading presented in Figure 4.

In addition, when the *i*/*n* grading width increased from 0 to 100 nm, the J_{SC} increased significantly from approximately 15 to 16 mA/cm^2 and the FF increased from 0.56 to 0.61 accordingly. The increase in J_{SC} and FF suggested that the *i*/*n* grading enhanced the carrier collection in the absorber. Presumably, the potential gradient created by the *i*/*n* grading

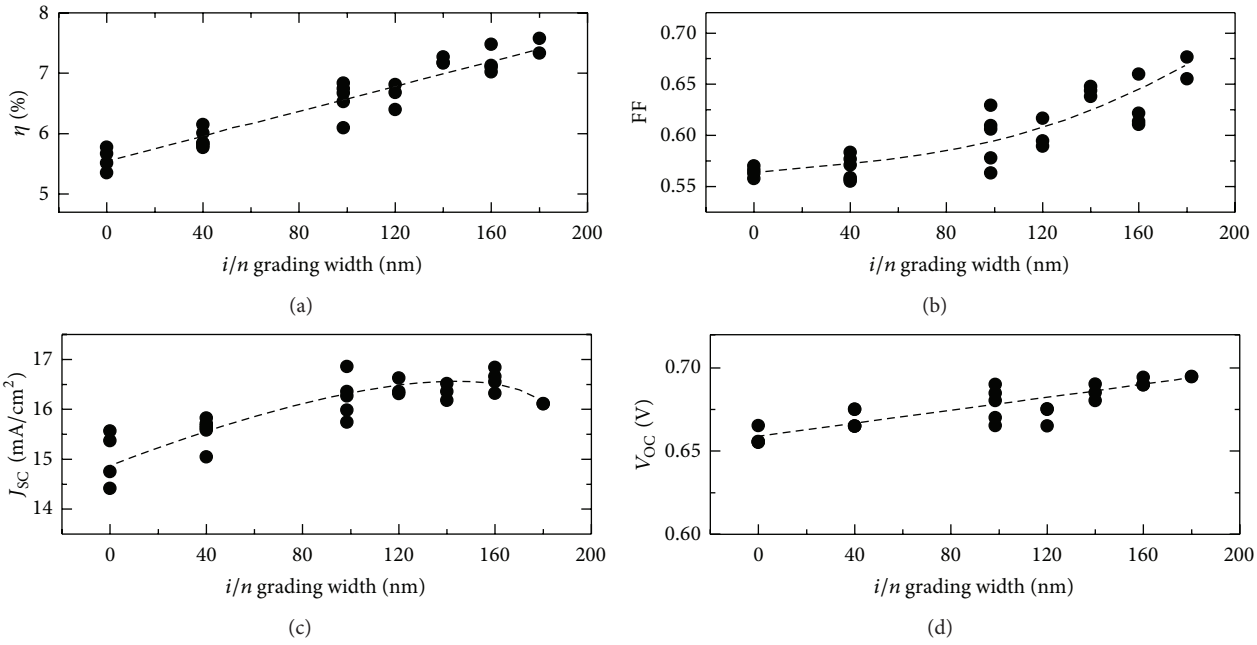

FIGURE 6: The performance of a-$Si_{1-x}Ge_x$:H single-junction cells as a function of the *i/n* grading width under illumination of AM1.5G light source. The *p/i* grading width and the total thickness of absorber were 15 and 230 nm, respectively, for all the cells. The lines were drawn to guide the eye.

facilitated the hole transport and also strengthened the built-in electric field in the absorber [12, 14]. As the *i/n* grading width increased from 100 to 160 nm, the J_{SC} seemed saturated at approximately 16.5 mA/cm^2 while the FF increased from 0.61 to 0.65 monotonically. The increased FF suggested that the carrier collection was further improved by the *i/n* grading. The saturated J_{SC} was due to the cancellation of improved EQE at wavelength from 650 to 750 nm and the reduced EQE from 750 to 900 nm as shown in Figure 5. Further increase in the *i/n* grading width to 180 nm improved the FF to 0.66 while reducing J_{SC} to 16.1 mA/cm^2 due to the reduced longer-wavelength response. The cell efficiency improved significantly from 5.5% to 7.5% as the *i/n* grading width increased from 0 to 180 nm. However, since a-$Si_{1-x}Ge_x$:H cells were generally used as bottom cells, thicker *i/n* grading width would lead to substantial reduction in long-wavelength response which may be potentially unfavorable in the tandem cell design. As a result, the *i/n* grading should be as thick as 100 to 160 nm to take advantage of the improved carrier collection meanwhile minimizing the reduction in longer-wavelength response.

Figure 7 compares the EQEs of a-$Si_{1-x}Ge_x$:H cells with and without bandgap graded layers measured under different bias voltages. The cell without bandgap grading exhibited substantially larger increase at wavelength from 400 to 900 nm under −0.5 V bias. In contrast, the cell employing bandgap graded layers showed only marginal increase in EQE under −0.5 V at wavelength from 450 to 700 nm, which suggested that most carriers were extracted under short-circuit condition. This result suggested that the bandgap graded layers improved the carrier collection significantly and thus can make a more efficient light management in a-$Si_{1-x}Ge_x$:H

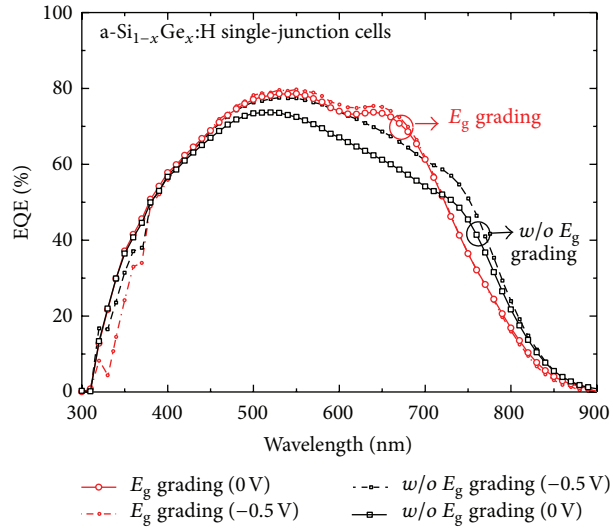

FIGURE 7: Comparison between EQEs of a-$Si_{1-x}Ge_x$:H single-junction cells with and without bandgap graded layers at the *p/i* and the *i/n* regions. The circle and square symbols denote the cell with and without bandgap grading, respectively. The *p/i* and *i/n* grading widths and the total thickness of absorber were 15, 160, and 230 nm, respectively. The EQEs measured under reverse bias of −0.5 V were represented by the dash lines.

cells. On the other hand, the reduction in the EQE at wavelength below 400 nm with reverse bias was probably due to the electron collection issues or the signal instability of the EQE system under biased condition. Further exploration on the nonlinear bandgap grading profiles shall lead to enhanced longer-wavelength response.

4. Conclusions

In this work, the effect of bandgap grading of absorbers on the performance of a-$Si_{1-x}Ge_x$:H cells employing μc-SiO_x:H *n*-layer was investigated. The influence of the *p/i* and the *i/n* grading widths on carrier collection and photon absorption in the cells was evaluated by the bias-dependent EQE measurement, the total reflection spectra of cells, and the *J-V* characteristics. The cell employing 20 nm thick *p/i* grading improved the V_{OC} by 0.4 V, which was 6.3% relative increment compared to the cell without grading. The *p/i* grading seemed to reduce the interface defects as evidenced by the decreased dark leakage current. On the other hand, the cell with 160 nm thick *i/n* grading relatively enhanced the V_{OC}, J_{SC}, FF, and efficiency by 5.0%, 10.4%, 11.0%, and 28.7%, respectively, compared to the cell without *i/n* grading. The bias-dependent EQE manifested that the carrier collection was significantly improved which was likely due to the facilitation of hole transport. One trade-off was the long-wavelength response reduced with the increasing of *i/n* grading width. Compared to the cell without grading, the a-$Si_{1-x}Ge_x$:H cells with optimal *p/i* and *i/n* grading widths improved the efficiency from 5.5 to 7.5%.

Conflict of Interests

The authors do not have any conflict of interests concerning the content of the paper.

Acknowledgment

This work was financially sponsored by the National Science Council under Grant no. 102–3113-P-008-001.

References

[1] S. Guha, J. S. Payson, S. C. Agarwal, and S. R. Ovshinsky, "Fluorinated amorphous silicon-germanium alloys deposited from disilane-germane mixture," *Journal of Non-Crystalline Solids*, vol. 97-98, no. 2, pp. 1455–1458, 1987.

[2] B. Yan, G. Yue, L. Sivec, J. Yang, S. Guha, and C. S. Jiang, "Innovative dual function nc-SiO_x:H layer leading to a >16% efficient multi-junction thin-film silicon solar cell," *Applied Physics Letters*, vol. 99, no. 11, Article ID 113512, 2011.

[3] A. Lambertz, T. Grundler, and F. Finger, "Hydrogenated amorphous silicon oxide containing a microcrystalline silicon phase and usage as an intermediate reflector in thin-film silicon solar cells," *Journal of Applied Physics*, vol. 109, no. 11, Article ID 113109, 2011.

[4] A. Lambertz, V. Smirnov, T. Merdzhanova et al., "Microcrystalline silicon-oxygen alloys for application in silicon solar cells and modules," *Solar Energy Materials and Solar Cells*, vol. 119, pp. 134–143, 2013.

[5] P. Buehlmann, J. Bailat, D. Dominé et al., "In situ silicon oxide based intermediate reflector for thin-film silicon micromorph solar cells," *Applied Physics Letters*, vol. 91, no. 14, Article ID 143505, 2007.

[6] C. Das, A. Lambertz, J. Huepkes, W. Reetz, and F. Finger, "A constructive combination of antireflection and intermediate-reflector layers for thin film solar cells," *Applied Physics Letters*, vol. 92, no. 5, Article ID 053509, 2008.

[7] V. Smirnov, W. Bottler, A. Lambertz, H. Wang, R. Carius, and F. Finger, "Microcrystalline silicon n-i-p solar cells prepared with microcrystalline silicon oxide (μc-SiO_x:H) n-layer," *Physica Status Solidi C*, vol. 7, no. 3-4, pp. 1053–1056, 2010.

[8] P. Delli Veneri, L. V. Mercaldo, and I. Usatii, "Silicon oxide based n-doped layer for improved performance of thin film silicon solar cells," *Applied Physics Letters*, vol. 97, no. 2, Article ID 023512, 2010.

[9] H.-J. Hsu, S.-W. Liang, C.-H. Hsu, and C. C. Tsai, "Optical enhancement in a-Si:H/a-SiGe:H tandem and a-SiGe:H single-junction solar cells," in *Proceedings of the 25th International Conference on Amorphous and Nano-Crystalline Semiconductors (ICANS-25 '13)*, Toronto, Canada, August 2013.

[10] S. Guha, J. Yang, A. Pawlikiewicz, T. Glatfelter, R. Ross, and S. R. Ovshinsky, "Band-gap profiling for improving the efficiency of amorphous silicon alloy solar cells," *Applied Physics Letters*, vol. 54, no. 23, pp. 2330–2332, 1989.

[11] B. E. Pieters, M. Zeman, R. A. C. M. M. van Swaaij, and W. J. Metselaar, "Optimization of a-SiGe:H solar cells with graded intrinsic layers using integrated optical and electrical modeling," *Thin Solid Films*, vol. 451-452, pp. 294–297, 2004.

[12] F. Rubinelli, R. Jiménez, J. Rath, and R. Schropp, "Using computer modeling analysis in single junction *a*-SiGe:H solar cells," *Journal of Applied Physics*, vol. 91, no. 4, article 2409, 2002.

[13] R. J. Zambrano, F. A. Rubinelli, W. M. Arnoldbik, J. K. Rath, and R. E. I. Schropp, "Computer-aided band gap engineering and experimental verification of amorphous silicon-germanium solar cells," *Solar Energy Materials and Solar Cells*, vol. 81, no. 1, pp. 73–86, 2004.

[14] J. Zimmer, H. Stiebig, and H. Wagner, "a-SiGe:H based solar cells with graded absorption layer," *Journal of Applied Physics*, vol. 84, no. 1, pp. 611–617, 1998.

[15] E. Maruyama, Y. Yoshimine, A. Terakawa et al., "Improvement in performance of a-SiGe:H solar cells for multi-junction cells," in *Proceedings of the MRS Spring Meeting*, pp. 821–826, April 1993.

[16] X. Deng, X. Liao, S. Han, H. Povolny, and P. Agarwal, "Amorphous silicon and silicon germanium materials for high-efficiency triple-junction solar cells," *Solar Energy Materials and Solar Cells*, vol. 62, no. 1, pp. 89–95, 2000.

[17] J. Tauc, "Optical properties and electronic structure of amorphous Ge and Si," *Materials Research Bulletin*, vol. 3, no. 1, pp. 37–46, 1968.